ngravs: Distinct gravitational interactions in GADGET-2

K. A. S. Croker[a]

[a]*Department of Physics and Astronomy, University of Hawai'i at Mānoa, 2505 Correa Road, Honolulu, HI., USA*

arXiv:1502.07442v2 [astro-ph.IM] 9 Jun 2016

Abstract

We discuss an extension of the massively parallel cosmological simulation code GADGET-2, which now enables investigation of multiple and distinct gravitational force laws, provided they are dominated by a constant scaling of the Newtonian force. In addition to simplifying investigations of a universally modified force law, the *ngravs* extension provides a foundation for state-of-the-art collisionless cosmological simulations of exotic gravitational scenarios. We briefly review the algorithms used by GADGET-2, and present our extension to multiple gravities, highlighting additional features that facilitate consideration of exotic force laws. We discuss the accuracy and performance of the *ngravs* extension, both internally and with an unaltered GADGET-2, in the relevant operational modes. The *ngravs* extension is publicly released to the research community.

Keywords: numerical methods, gravitation, cosmology, n-body

PROGRAM SUMMARY

Manuscript Title: ngravs: Distinct gravitational interactions in GADGET-2
Authors: K. A. S. Croker
Program Title: Gadget-2.0.7-ngravs
Journal Reference:
Catalogue identifier:
Licensing provisions: GNU General Public License v2
Programming language: C
Computer: Commodity
Operating system: Unix
RAM: 256MB+
Number of processors used: MPI
Keywords: numerical methods, gravitation, cosmology, n-body
Classification: 1.9 Cosmology, 4.12 Other Numerical Methods
External routines/libraries: Same requirements as GADGET-2
Nature of problem:
N-body cosmological codes are traditionally designed to investigate a single gravitating species interacting via the Newtonian force law. There exist viable extensions to General Relativity[1], however, which predict weak-field, slow-motion limits featuring distinct gravitational force laws between distinct particle species. To enable investigation and constraint of these theories with available astrophysical data, a necessary first step is to extend an N-body simulator to handle distinct gravitating species.
Solution method:
The massively parallel Barnes-Hut tree, Fast Fourier Transform, and sorting routines of the versatile and well vetted N-body simulator[2] GADGET-2 were extended to support D distinct gravitationally interacting species. The tree implementation now vectorizes over each species' monopole masses and positions, the Fourier routines now handle active and passive gravitational masses separately, and the sorting routines now group all particle data by type. The appropriate TreePM adjusted forces are computed via FFT and tabulated before runtime. An additional file was introduced allowing the user to specify all D^2 gravitational interactions: real space, Fourier space, and lattice summation corrections. To improve monopole approximations in scenarios where the scale of the gravitational interaction depends on the mass itself, an optional tracking of the number of bodies contributing to any particular monopole approximation has been written.
Restrictions:
Mesh methods with non-periodic boundary conditions have been disabled. Force laws with mass dependent scale lengths are not amenable to the implemented Fourier methods (or even the traditional[3] Fourier approach). Nodes containing highly heterogeneous collections of particles with different mass dependent scale lengths may not be well-approximated, even with the additional tracking introduced. The collisional "gas" species can only interact via a single gravitational force law.
Unusual features:
The extension allows simultaneous consideration of at most six distinct central forces, where each is a sum of bounded, monotonic, gradients of radially modulated Newtonian potentials. This will serve as a common platform for model-dependent adjustments to the cosmological background evolution.
Additional comments:
Data file format is identical to that of GADGET-2. Configuration file format is unchanged, save for the addition of required bindings between particle species and gravitational type. To install ngravs, first install GADGET-2 (available at http://www.mpa-garching.mpg.de/gadget/), then replace the contents of the Gadget2 subdirectory with the files included in the provided tarball. Alternatively, one can clone the github repository https://github.com/kcroker/Gadget-2.0.7-ngravs and provide one's own configuration and initial data files.
Running time:
Typical running times are $\lesssim 2D\times$ those of GADGET-2, where D is an integer between 1 and 6.

Email address: kcroker@phys.hawaii.edu (K. A. S. Croker)

References

[1] V. Springel, The cosmological simulation code GADGET-2, MNRAS 364 (2005) 1105–1134. arXiv:astro-ph/0505010, doi:10.1111/j.1365-2966.2005.09655.x.

[2] M. Hohmann, M. N. R. Wohlfarth, Repulsive gravity model for dark energy, Phys. Rev. D81 (10) (2010) 104006. arXiv:1003.1379, doi:10.1103/PhysRevD.81.104006.
Reference 2

[3] R. W. Hockney, J. W. Eastwood, Computer Simulation Using Particles, IOP Publishing Ltd, 1988.

1. Introduction

At present, there is substantial evidence that most of the mass and energy within our universe is non-luminous. Big bang nucleosynthesis and baryon acoustic oscillations strongly constrain[1] the fraction of non-luminous matter with respect to the luminous component from the radiation dominated era onward. Yet, while they and other evidence, such as the Bullet Cluster[2], strongly suggest that the dark fraction can be well-approximated by pressureless ideal fluid, the composition and precise distribution of this dark matter is far from clear. While numerous particle dark matter candidates[3] are theoretically popular at present, conflicting exclusions from possible detections and increasingly stringent constraints from lack of direct detection[4] at cosmologically desirable mass scales continue to motivate investigation in novel directions.

With the growing wealth of high-precision astrophysical data[5–7] and the absence of a "bottom-up" understanding of dark matter, N-body methods[8] have become essential for comparison against highly non-linear theoretical predictions in structure formation over many decades of spatio-temporal scale. In the past twenty years, the sophistication of such cosmological simulations both in physical scope and technical implementation has undergone unprecedented growth[9–11]. While significant literature exists on the use of N-body methods to explore standard structure formation scenarios, there exist proposed exotic scenarios that are also amenable to N-body methods. In a particularly intriguing case, Hohmann & Wohlfarth[12] proposed to model Dark Energy as a *repulsive* gravitational interaction between matter species belonging to distinct copies of the Standard Model. This model should make very strong predictions for weak-lensing observations and could be readily adapted to the dark matter problem. This motivates the extension of existing numerical simulation tools to investigate and constrain more general cosmological models.

One well-established and versatile simulation tool is GADGET-2: a massively parallel code with extensive memory and speed optimization employed both algorithmically and architecturally[13]. GADGET-2 has been extended to consider three distinct gravitationally interacting species by Baldi et. al. [14] to enable investigation of coupled dark-energy cosmologies. Unfortunately, their extension is focused on particular cosmological models and not publicly available.

In the following, we discuss our independent and augmented implementation of D distinct gravitationally interacting species in GADGET-2. To facilitate investigation of models amenable to multi-species treatments by individual researchers, our publicly released *ngravs* extension permits convenient definition of D^2 distinct gravitational force laws and optionally provides additional data which can be used to improve force accuracy under certain scenarios. Our primary aim is to facilitate large scale structure investigations of multi-species models, with considerable freedom in the precise form of the gravitational force laws. Our initial use of *ngravs* will be the constraint of such models through predicted galaxy power spectra.

We assume the reader is familiar with the goals, construction, and operation of modern N-body codes. Throughout this paper, D will always refer to the number of distinct gravitationally interacting species, while N will refer to the number of bodies considered in any particular simulation. Units will be such that $G \equiv c \equiv 1$. Stock will refer to the unaltered GADGET-2.0.7 code, while *ngravs* will refer to our augmented version of this same code.

2. Implementation

The algorithms employed by GADGET-2 to compute collisionless forces are a Barnes-Hut tree walk and, optionally, a particle mesh (PM) computation. To construct the tree, the simulation volume is recursively halved until each particle resides within its own leaf. Interparticle forces are then computed for any specific particle by recursive traversal of the tree, halted when a monopole approximation of the force from all deeper branches satisfies a user-specified force accuracy "opening criterion." PM forces are computed by interpolating particle positions to a mass density defined on a regular grid, performing a Fourier transformation, convolving with the k-space Greens' function, and inverting the transform. The resulting potential is then interpolated back to forces at all particle positions. The tree algorithm may be used exclusively, or can be combined with the PM algorithm in a hybrid arrangement (TreePM) where the tree is used to compute short range forces, and the PM algorithm used to rapidly compute distant contributions. In TreePM mode, the k-space Greens' function is Gaussian filtered, and the corresponding truncated short range force is summed with a spatially restricted Tree walk. The GADGET-2 code is engineered so that tree and PM computations are nearly decoupled from the more intricate collisional force computations, time integration, parallelization decomposition, and IO routines. This permits a targeted and straight-forward extension to multiple gravitational interactions.

GADGET-2 implements 6 distinct particle types, including a "gas" type which features additional force compu-

Table 1: Time averaged $D = 1$ and $D = 3$ *ngravs* tree computation performance with Newtonian interactions, normalized to stock runtimes. $\dot{N}$ represents particles processed per second, adjusted for interprocess communication delays. Subscript labels indicate stock (stc) or *ngravs* ($D = 1, 3$). Note that the purely collisional gas sphere cannot be tested for $D > 1$ (see § 2.5).

Test case	$\left\langle \dot{N}_{D=1} \right\rangle / \left\langle \dot{N}_{\rm stc} \right\rangle$	$\left\langle \dot{N}_{D=3} \right\rangle / \left\langle \dot{N}_{\rm stc} \right\rangle$
Galaxy collision	0.706	0.334
ΛCDM gas	0.779	0.405
Gas sphere	0.759	-

tations from collisional dynamics. Let $1 \leq D \leq 6$ be the number of distinct gravitational species. For particle types i, j, the following map is established between $0 \leq i, j \leq K \equiv D - 1$ generalizing Newton's law of gravitation

$$\vec{F}(m_i, M_j, r, N_\perp) = -\frac{m_i M_j}{r^2}\hat{r} \longrightarrow f_{ij}(r, N_\perp)\hat{r} \quad (1)$$

Here each f_{ij} is dominated by a constant scaling of the Newtonian force, with specific forms detailed in §2.1. They depend on the separation of masses r, the active mass M_j, the passive mass m_i, and the number of source particles $N_\perp$ contributing to the monopole approximation employed by the Barnes-Hut tree algorithm. In the direct force case, $N_\perp \equiv 1$.

As the standard Newtonian force diverges as $r \to 0$, in order to maintain numerical accuracy under reasonable timesteps, GADGET-2 artificially smooths to zero the gravitational interaction below some (type dependent) length scale. In general, D^2 distinct "softenings" analogous to (1) must also be specified. We have implemented the above mappings through function pointers, enabling much model-dependent code to be conveniently populated within a single location. Thus, at the user's option, tables for the gravitational potential, $\vec{k}$-space Greens' functions, and lattice sum corrections may also be specified as desired.

Pure tree computations have been extended to both periodic and non-periodic modes, while TreePM computations have been extended only to periodic mode at present, removing the possibility of secondary PM "zoom" simulations from the *ngravs* extension. For justification of this design choice, we direct the reader to § 2.5.

Performance comparisons with respect to stock can be found in Table 1, where we find an ∼40% increased runtime due to additional overhead within the tree algorithm. It should be noted that the simulation specific performance of *ngravs*, apart from this constant scaling, is unchanged from that of stock. Thus, in $D = 1$ cosmological scenarios, the *ngravs* extension enables convenient investigation of a single, globally modified force law; if one can afford modestly longer runtimes. More importantly, the structures containing data on all N simulation particles are unchanged and so the favorable memory storage requirements of GADGET-2 are maintained.

2.1. Specific forms of f_{ij}

The Barnes-Hut algorithm makes assumptions about the nature of the force law which must be honored to maintain accuracy of the algorithm. This is not a serious impediment, as arbitrary forces are not relevant for cosmological investigations. We now develop properties of the f_{ij} which will permit investigation of a very wide range of possible scenarios, while simultaneously maintaining the established force accuracies of GADGET-2.

Investigations of the gravitational force between baryonic matter strongly constrain this interaction to an inverse-square law (ISL)[15]. Analogous constraint for dark matter, however, must presently come from large scale astrophysical data. This leaves margin for speculation and motivates modification to the gravitational interaction of the dark component. Two popular deviations from the *baryonic* ISL, in the notation of [15], are the Yukawa-like

$$\vec{F}(r) = GMm\frac{\mathrm{d}}{\mathrm{d}r}\frac{1}{r}\left[C + \alpha \exp\left(\frac{-r}{\lambda}\right)\right]\hat{r} \quad (2)$$

and power-law

$$\vec{F}(r) = GMm\frac{\mathrm{d}}{\mathrm{d}r}\frac{1}{r}\left[C + \alpha\left(\frac{r_0}{r}\right)^{M-1}\right]\hat{r}. \quad (3)$$

We introduce the parameter $C \in \{0, 1\}$ to permit consideration of a "pure Yukawa" law as could present in massive gravity theories[16] or a harder power law, which would follow from dimensional considerations if point-like dark matter interactions were well-approximated by a Poisson law in greater than 3 non-compact spatial dimensions. Note that Equations (2) with $C \equiv 1$ and (3) strengthen the force law at small scales.

One may also consider the usual Newtonian force, but construct "effective" point-like force laws for extended mass distributions which remain rigid on dynamical timescales. An example could be a dark matter "particle" sourced by a non-pointlike mass density $\rho(r)$, stable on timescales relevant to simulation length. Such objects could be used to reduce particle count in a simulation, or to investigate novel approaches to the missing satellites[17] and "core cusp"[18] problems. These objects would interact with the usual baryonic matter via the following force

$$\vec{F}(r) = GMm\frac{\mathrm{d}}{\mathrm{d}r}\left[\frac{1}{r}\int_0^r \rho(r')r'^2\mathrm{d}r'\right]\hat{r} \quad (4)$$

where the integral must remain finite as $r \to \infty$. Note that, in contrast to the above force laws with $C = 1$, Equation (4) diminishes the force law at all scales.

Equations (2), (3), and (4) all take the form of the gradient of a modulated Newtonian potential

$$\vec{F}_{ij}(r) = m\frac{\mathrm{d}}{\mathrm{d}r}\frac{Ms_{ij}(r)}{r}\hat{r} \equiv -m\frac{\mathrm{d}}{\mathrm{d}r}V_{ij}(r)\hat{r} \quad (5)$$

where M is the active gravitational mass, $s_{ij}(r)$ is bounded, positive, and $\lim_{r\to\infty} s_{ij}(r)$ monotonically approaches a constant value. In the following discussion, we restrict our consideration to this class of force laws. We emphasize that M and must appear as a multiplier in order to maintain the superposition required by both the Tree and PM methods. It is assumed that the Equivalence Principle holds[19], and so m must also appear as a multiplier. We will now drop this passive/inertial mass and consider the accelerations a_{ij} when convenient.

For cosmological simulations of metric theories of gravity, the evolution of the scale factor is determined by the full field equations. Contributions to the weak field equations atop this Robertson-Walker background are then determined by first order perturbation theory. While one can now investigate significantly more general force laws below the horizon scale, if the background expansion is significantly altered from the Friedmann equations, additional adjustment to the timestep routines may be required to obtain meaningful numerical results on cosmological scales. Such modifications are beyond the scope of the present work.

2.1.1. Timesteps

The determination of a suitable timestep for the numerical integration is a subtle problem[20]. On the one hand, it is desirable to use the largest possible timestep to speed the simulation, but one must do so while maintaining force accuracy. In general, the larger the force, the smaller the required timestep. Though there are many approaches to determining a timestep[21], most require knowledge of higher derivatives and would require significant departure from the existing GADGET-2 code. We thus implement a minimal departure from the algorithm of GADGET-2. This guarantees the established force accuracy of GADGET-2 and facilitates comparision with studies performed with stock.

In the simplest scenario, GADGET-2 maintains sympletic time evolution by synchronously stepping each particle by

$$\Delta t_{\rm grav} = \min\left[\Delta t_{\rm max}, \left(\frac{2\eta\epsilon}{|\vec{a}|}\right)^{1/2}\right] \qquad (6)$$

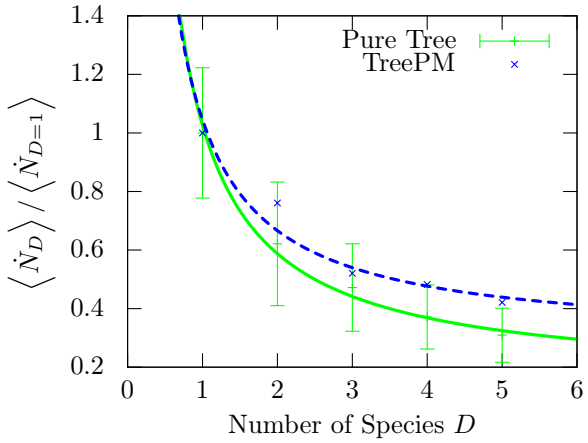
with η a user-specified dimensionless accuracy, $\vec{a}$ the particle's acceleration, and ϵ a user-specified gravitational softening length. The maximum timestep $\Delta t_{\rm max}$ is either specified by the user, or determined in cosmological simulations by enforcing that rms displacement should be well below mean particle separation. Though the nonphysical ϵ enters the timestep computation, this timestep has been shown to be robust for Newtonian interactions through numerical investigations[22].

To *guarantee* the already established force accuracy of GADGET-2 without alteration of the time integration algorithms, we note that the permissible f_{ij} exhibit an $A_{\rm max}$ such that the accelerations a_{ij} are bounded by $A_{\rm max}/r^2$, provided one remains outside of an appropriately defined softening scale. Thus, we may modify Equation 6 by a constant scaling

$$\Delta t_{\rm grav} = \min\left[\Delta t_{\rm max}, \left(\frac{2\eta\epsilon}{A_{\rm max}\,|\vec{a}|}\right)^{1/2}\right]. \qquad (7)$$

This works because any acceleration smaller than that due to this scaled Newtonian force will produce smaller adjustments to any trajectory per unit time, and thus will be tracked to greater precision by the existing timestepping algorithms.

Figure 1: Average particles processed per second $\dot{N}$ given D species, normalized to $D = 1$. Curves are separate one-parameter fits cx^{-1} to the data. Note the decrease proportional to D^{-1} as expected in both pure tree and TreePM modes. Rather large error bars for the TreePM scenario have been omitted for clarity as the relevant quantity is average performance.



2.2. Tree forces

In keeping with our approach, the existing tree routines were extended simply by vectorizing over the monopole mass centers and velocities. This additional data increases tree memory consumption by $\sim 0.3(D-1)$ from stock. In order to accommodate more exotic force laws for which the interaction scale is related to the active gravitational mass in more complicated ways, the tree structure and construction were augmented to optionally track $N_\perp$ for all contributing types. This quantity can then be used to suitably correct computation of the monopole moment.

During force computation, tree walks may be significantly optimized by suitable choice of opening criteria. For collisionless force computations in stock, the tree is traversed at most twice, once for the usual particle-particle interaction, and once again for any periodic correction. The latter walk can proceed more efficiently, as the opening criteria is significantly different: corrections to near particles are very small. We considered performing D separate tree walks, but stock employs a very effective relative opening criteria during the tree walk, where the acceleration previously computed is compared to a Newtonian estimate of the new acceleration to determine whether to traverse the

branch. These previous accelerations, however, are stored on a per-particle basis and the amount of memory required to store $D-1$ additional accelerations produced an unacceptable increase in memory consumption. It was decided that, since many alternative force-laws cannot deviate too strongly from the Newtonian force, any gains in speed due to decreased depth within the tree would not be offset by the additional memory requirement. Instead, we vectorized within the single tree walk that GADGET-2 already performs, and continue to employ the Newtonian relative opening criteria. This opening criteria is conservative, provided that the alternative force-laws are dominated by the usual Newtonian interaction. This results in slightly improved force errors that can be easily understood: in a limit where the mass distribution is characterized by N distinct monopoles, one simply regenerates the exact force. Overall, the tree walk runtime increases by a factor of D. Indeed such behavior is found in Figure 1, where the average number of particles processed per second decreases as $1/D$.

2.3. Lattice corrections

Stock periodic computations may optionally proceed in pure tree mode with the method of Ewald summation[23]. The Ewald technique is a specific application, to the ISL, of methods designed to transform poorly convergent sums of periodic images in r-space into rapidly convergent sums in k-space. These methods belong to the broader topic of lattice sums[24] which are, in general, challenging to compute. In terms of error functions, computation can be reduced to quadrature[25], with the usual caveats that apply to numerical integration. *ngravs* can tabulate given corrections from an infinite image lattice for each of D^2 direct forces, and interpolate to actual particle positions in the same manner as stock. In practice, the lattice correction is usually specified as a consistency check against the Fourier computations, and not used in actual simulations.

2.4. PM forces

In order to minimize surface to volume ratio, stock does not attempt to overlap local PM computation with local particle distribution. Instead, density data is exchanged between all parallel processes according to an optimal slab decomposition determined by the Fast Fourier Transform (FFT) routines[26], and the resulting potential is exchanged back. Since the identities of all the particles which contribute to any given slab are unknown, the PM routine must iterate D^2 times (instead of $D(D+1)/2$ and exploiting symmetry), so that each gravitational type can be both the passive and active gravitational mass. Though more sparse, the exchanged data is of the same dimension and the runtime increases by a factor of D^2. This performance degradation is of little concern, however, as the FFT runtime continues to be heavily subdominant to that of the Tree algorithm, as is clear in Figure 1.

In GADGET-2, one may optionally enable Peano-Hilbert sorting of particle data on each local processor. This was found by Springel[13] to often give substantial (but architecture dependent) improvements in runtime as spatial proximity translates to memory proximity. To enable processing of the entire local particle content with only a single traversal of the data, if $D > 1$ and TreePM mode is enabled, we have implemented an additional sort by gravitational type before the Peano-Hilbert sort. Subsequently, each gravitational type is then Peano-Hilbert sub-sorted. As is done in stock, both sorts proceed so that only one reordering of the particle data memory is required. For compatibility with the collisional code of GADGET-2, collisional particles must be mapped to gravitational type zero.

2.4.1. TreePM short-range forces

In the hybrid TreePM mode, stock applies a Gaussian low-pass filter to the k-space Newtonian potential. This permits highly accurate and rapid computation of a long-range Coloumb force with the PM algorithm. On spatial scales near a user-specified a_{smth} number of mesh cells, the short-range force is calculated by smoothly transitioning to a partial tree walk using a suitably adjusted potential

$$\phi^{\text{short}}(r) \equiv \mathscr{F}^{-3}\left\{\phi_k\left[1-\exp\left(-k^2 r_s^2\right)\right]\right\} \tag{8}$$

and taking a radial derivative, where $\mathscr{F}^{-3}$ denotes the 3D inverse Fourier transform, and $r_s \equiv 2\pi a_{smth}/L$. It is a convenient coincidence that, in the Newtonian case, this Fourier transform yields $\phi^{\text{short}}(r) = \phi(r)\text{erfc}(r/2r_s)$. Stock samples a user-specified number N_{TAB} of this factor and its derivative, and then multiplies the computed tree potential and force by these respective modulations. For the case of a general force-law, we consider instead

$$\phi_{ij}^{\text{short}}(r) = \phi_{ij}(r) - \frac{2\pi}{r}\int_0^r \mathscr{F}_{r'}^{-1}\left\{\bar{\phi}_{ij}(k)\exp(-k^2 r_s^2)\right\}\,\mathrm{d}r' \tag{9}$$

where we have performed the angular integrations of the transform. We have also well-conditioned the computation by taking a derivative with respect to r, and writing

$$\bar{\phi}_{ij}(k) \equiv k^2\phi_{ij}(k) \tag{10}$$

which is just $\phi_{ij}(k)$ normalized by the Newtonian Greens' function. This lessens the severity of singularities in $\phi_{ij}(k)$ before computation due to our prior constraint of the f_{ij}.

Subtractions, such as in Equation 9, which involve two values very near unity can suffer from loss of precision. We note, however, that the Fourier integrand of Equation 9 is effectively band-limited, so its values may be rapidly and precisely (to near machine precision) computed during initialization of *ngravs* by an inverse FFT. The acceleration is found from differentiation of Equation 9 with respect to r

$$\begin{aligned} a_{ij}^{\text{short}}(r) =& a_{ij}(r) - \frac{2\pi}{r^2}\int_0^r \mathscr{F}_{r'}^{-1}\left\{\bar{\phi}_{ij}(k)\exp(-k^2 r_s^2)\right\}\,\mathrm{d}r' \\ &+ \frac{2\pi}{r}\mathscr{F}_r^{-1}\left\{\bar{\phi}_{ij}(k)\exp(-k^2 r_s^2)\right\}. \end{aligned} \tag{11}$$

To maintain requisite precision during the computation, the integration in r-space is performed using a 4-point Newton-Cotes formula, giving an error for the integration bounded by

$$< \left(\frac{r_s}{10 N_{\mathrm{TAB}} \mathscr{O}}\right)^5 \partial_r^3 \mathscr{F}_r^{-1} \left\{\bar{\phi}_{ij}(k) \exp\left[-k^2 r_s^2\right]\right\}$$
$$< \frac{r_s}{\left(10 N_{\mathrm{TAB}} \mathscr{O}\right)^5} \quad (12)$$

where $\mathscr{O} \in \mathbb{N}$ is a user-specified parameter which controls the resolution of the FFT. The error bound in Equation 12 follows from application of standard inequalities and our constraint of the a_{ij}.

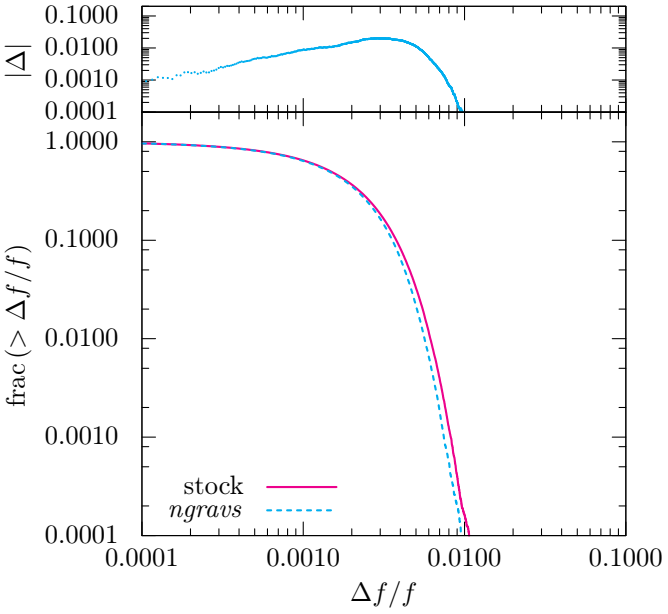
2.5. Limitations

Stock computes the non-periodic k-space Greens' function through explicit FFT of the sampled r-space potential on a mesh of twice the dimension desired for use in simulation. Unfortunately, generalization of this procedure from the specification of the periodic k-space Greens' function as is done in the accurate computation of the truncated short-range force is not practical due to memory constraint. Similarly, sampling the transformed radial function enough to guarantee the requisite accuracy on all points of the lattice through cubic interpolation encounters similar memory constraint. Since non-periodic computations may be performed to unlimited dynamic range with the extended Tree algorithm, and since large-scale investigations of modified force laws would naturally proceed investigations on smaller scales, we do not believe this to be a serious omission.

In GADGET-2, collisional forces are only computed for one type of "gas" particle. As highlighted by Marri & White[27], distinct gas species can allow the effective capture of a broad range of physical phenomena involved in galaxy formation and evolution. While it is possible to alter the gravitational force laws involving the gas, *ngravs* does not implement multiple gas species. This choice was one of simplicity and further extension to multiple gas species, i.e. following Scannapieco *et. al.*[28], is straightforward and could form the basis of future work.

At present, particle interactions under force laws with mass dependent scale are only accurately computed for uniformly massed gravitational species. This applies to both active and passive mass dependence. Without uniform masses, accurate computation is only possible only in pure tree, non-periodic mode. This is due to the Fourier computation's use of a single momentum-space Greens' function for all contributing densities, and to the necessary precomputation of force and potential correction tables for direct infinite lattice contributions. Even in non-periodic pure tree mode, due to the monopole averaging procedure, considerable force errors could result given situations where a node contains comparable numbers of same-species particles with different masses. The efficient and accurate computation of such interactions is an open question.

Figure 2: Fraction of forces computed during entire simulation with force error in excess of $\Delta f/f$, for Pure Tree mode and non-periodic boundary conditions, with $D = 3$ *ngravs* (blue, dashed). All interactions are Newtonian to permit direct comparison with stock (magenta, solid). Residuals $|\Delta|$ from stock shown at top. Note slightly improved force accuracy for *ngravs* due to more detailed characterization of the mass distribution.



3. Test problems

Since GADGET-2 has been well vetted over the past decade, to verify the correctness of the *ngravs* extension, it suffices to demonstrate that *ngravs* with Newtonian interactions and stock agree in their common operational modes. In addition to these consistency checks, we also investigate the TreePM and Pure Tree algorithms under more general force laws.

Profiling results presented in Table 1 and Figure 1 were carried out to double precision on a dedicated machine using 32 of 48 available cores for computation with 94 gigabytes of RAM. Periodic profiling and force accuracy runs were performed at double precision with a 128 point mesh. TreePM transition studies were performed on a 256 point mesh. Simulation initial conditions are those included with stock, with particle type reassigned as necessary to test *ngravs*. Our parameters can be found in Appendix Appendix A.

3.1. Comparison with stock

We present force accuracy comparisons between stock and $D = 3$ *ngravs* for two of the four stock included test initial conditions. In Figure 2, we demonstrate consistency with stock for pure tree operation under non-periodic boundary conditions. In Figure 3, we demonstrate consistency with stock for TreePM operation under periodic boundary conditions. This test verifies the correctness of the lattice summation, as the direct force computation requires the lattice correction under periodic

Figure 3: Fraction of forces computed during entire simulation with force error in excess of $\Delta f/f$, for TreePM mode and periodic boundary conditions, with $D = 3$ *ngravs* (blue, dashed). All interactions are Newtonian to permit direct comparison with stock (magenta, solid). Residuals $|\Delta|$ from stock shown at top. Note that an erroneous softening scale of 600kpc in the default stock ΛCDM initial condition was reduced to 50kpc to keep the softening scale below the cutoff for use of the PM computation.

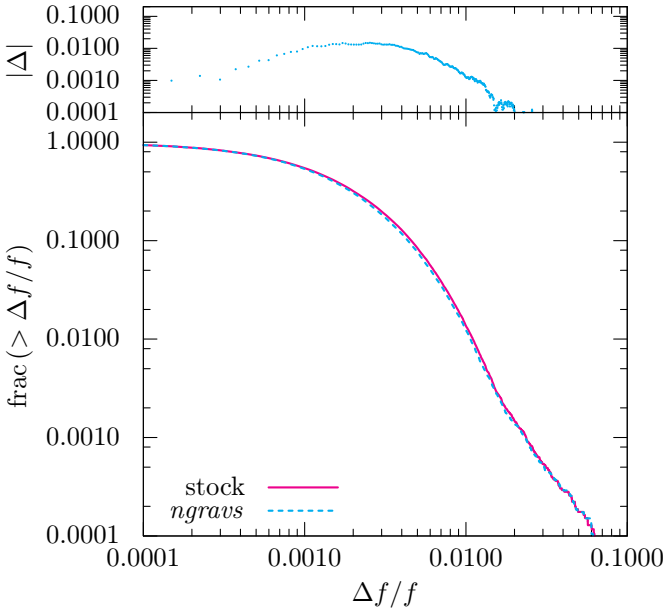
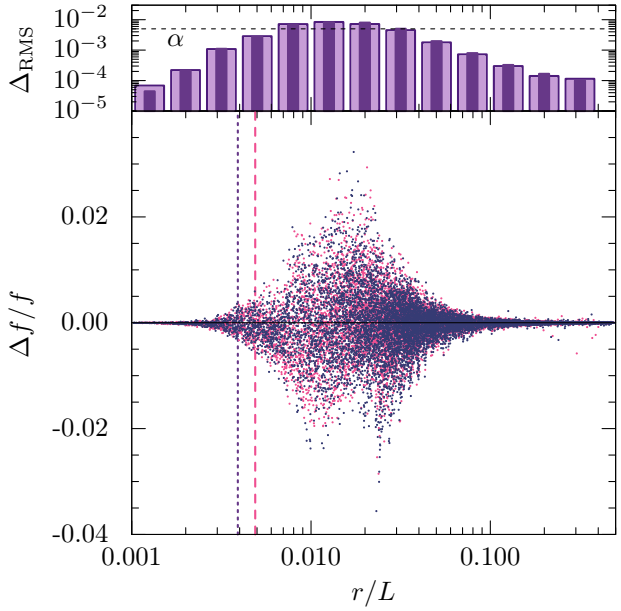


Figure 4: Force error as a function of separation for the Coloumb interaction with periodic boundaries. Stock is shown in red (grey), and *ngravs* $D = 1$ in blue (black). Errors stacked from ten distinct simulations of a randomly placed massive source interacting with randomly placed test particles. Vertical lines represent the mesh scale (dotted) and transition scale (dashed). Binned rms shown at top, with $\alpha \equiv 0.005$ the specified error tolerance for the tree algorithm.



boundary conditions. This periodic test also includs a collisional "gas" species, which further verifies the integrity of the unmodified collisional code. All figures display the fraction of force computations with force error

$$\Delta f/f \equiv \frac{\left|\vec{F}_{\rm alg} - \vec{F}_{N^2}\right|}{\left|\vec{F}_{N^2}\right|} \tag{13}$$

in excess of that fraction. Here, subscripts "alg" and N^2 represent computation by tree/mesh routines and direct Newtonian summation, respectively. The collapsing gas sphere was excluded as the present implementation of *ngravs* requires that all collisional particles be of the same gravitational species. Note that the force accuracies are virtually identical; favorable residuals indicate relatively minor improvements due to three multipole moments per node.

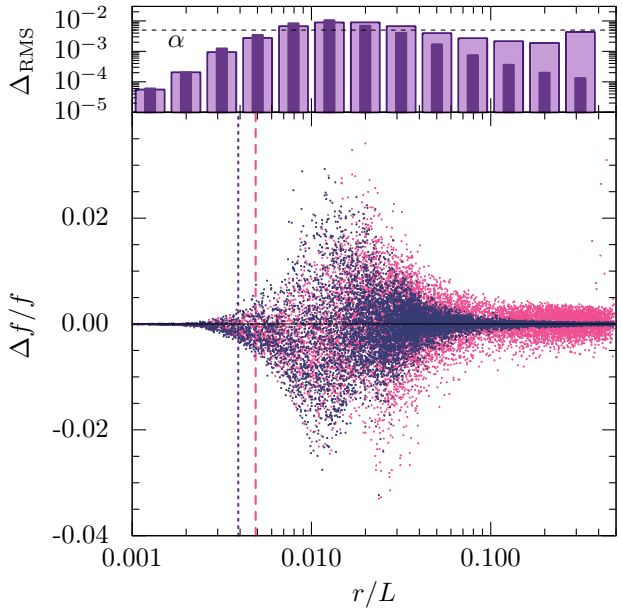
In addition to characterizing errors across entire simulations, we have also investigated the detailed error behavior of the TreePM algorithm in the transition region. We perform this test by creating a sequence of initial conditions each with a randomly placed massive source and shells of ~ 5000 randomly placed test particles. The test particle density drops as $1/r^3$ so that the number of interactions per shell is roughly constant. All particles have zero initial velocities and we consider only the first force computation, recording force errors for all interactions. The results of 10 of these runs are then stacked. Performance with the Newtonian interaction can be seen in Figure 4, where the force error behavior is indistinguishable from that of stock.

3.2. The pure Yukawa interaction

To verify correct and accurate behavior of the TreePM transition algorithm with more general forces, we have implemented the pure Yukawa (Yukawa) interaction. The Yukawa interaction represents a pathological "edge case" for the k-space Gaussian low-pass filter approach, because its r-space behavior is already exponentially suppressed before filtering. Conveniently, there exists significant literature on lattice sums involving the Yukawa potential, and our reference lattice implementation follows that of Salin and Caillol[29]. By comparison with a box filter, it was determined that the tree contribution remained non-negligible relative to the PM contribution under the Gaussian filter. Fortunately, we found that this pathology, specific to the Gaussian filter, can be corrected by simply scaling the Yukawa $\vec{k}$-space Greens' function by $\exp(-y_m^2 r_s^2)$ where y_m is the Yukawa field mass and r_s is the filter transition scale.

In Figure 5 we demonstrate the error performance for dimensionless $y_m \in \{10, 50\}$, with 50 sufficient to give eventual $10\times$ suppression of the Coloumb potential over the transition region. Note that the rms error is essentially unchanged throughout the transition region. The rms error at large r increases with increasing y_m due to the presence of additive exponential terms in the reference

Figure 5: Force error as a function of separation for the Yukawa interaction with periodic boundaries. Yukawa field masses $y_m = 10$ (blue, black) and $y_m = 50$ (pink, grey) shown. Errors for each field mass stacked from ten distinct simulations between a randomly placed massive source, with randomly placed test particles. Vertical lines represent the mesh scale (dotted) and transition scale (dashed). Binned rms shown at top, with $\alpha \equiv 0.005$ the specified error tolerance for the tree algorithm.



lattice sum and subsequent loss of precision. We note that this force test can be performed accurately in *ngravs* because the source and test masses can be assigned distinct gravitational types. Intra-type interactions can then be turned off completely. This is relevant for proper investigation of the pure Yukawa interaction, as exponential suppression makes nearer neighbors relevant, even with a very massive source.

In addition to pure Yukawa, we also have explored an evenly weighted sum of Yukawa and Coloumb to verify that our correction factor to Yukawa is robust. We find that the error performance is essentially unchanged from that of Coloumb, which verifies appropriate behavior in the transition region of the summed force.

3.3. The accumulator

To verify the newly introduced optional tracking of contributing particle counts $N_\perp$ in tree computations, we introduce a gravitational species where $N_\perp$ can be used to give an exact correction to the monopole approximation of the force laws. This test involves two species: species zero interacts via the usual Newtonian interaction

$$\Phi_{00}(r) = -\frac{M_0 m_0}{r} \tag{14}$$

where we use uppercase to denote the active gravitational mass and lowercase to denote the passive mass. The second species, denoted one, is characterized by a dimensionless scale β and interacts as

$$\Phi_{11}(r) = -\frac{2M_1 m_1}{\pi r} \tan^{-1}\left(\frac{4\pi\beta r}{M_1/N_\perp + m_1}\right). \tag{15}$$

Note that the interaction approaches Newton's at large r, but softens to a constant as $r \to 0$. This is the exact potential between two hypothetical, spherically symmetric, cored densities of the following form

$$\rho(r, M) = \frac{M^2}{4\beta\pi^3} \frac{1}{\left([M/2\beta\pi]^2 + r^2\right)^2} \tag{16}$$

where M is the total mass enclosed over all space by an object with density given by Eqn. 16. Interactions across species are of the same functional form as Eqn. 15, apart from the softening scale, which continues to be set by the cored object

$$\Phi_{10}(r) = -\frac{2M_0 m_1}{\pi r} \tan^{-1}\left(\frac{4\pi\beta N_\perp r}{m_1}\right) \tag{17}$$

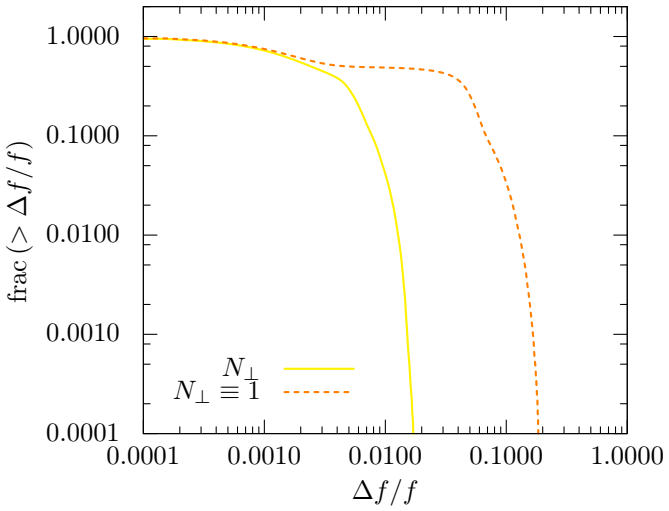
$$\Phi_{01}(r) = -\frac{2M_1 m_0}{\pi r} \tan^{-1}\left(\frac{4\pi\beta N_\perp r}{M_1}\right). \tag{18}$$

Note that Newton's third law is not violated, the distinct Eqns. 17 and 18 distinguish between the passive and active mass for correct computation. One may think of this interaction as a preference for phenomenological cored halos[18, 30] motivating a new class of hypothetical object, the Massive Astronomical Halo (Mahalo). The results in Figure 6 exhibit the force accuracy achieved through this novel $N_\perp$ feature.

4. Conclusion

We have detailed the *ngravs* extension to the massively parallel hybrid Tree and mesh N-body code GADGET-2, which now permits consideration of D^2 gravitational interactions between D particle species. Periodic simulations can proceed in either Tree or hybrid TreePM mode, while non-periodic simulations may be run in Tree mode. Our implementation vectorizes over the existing monopole moments within the Barnes-Hut tree, and distinguishes between active and passive gravitational mass during the mesh computations. Memory consumption remains favorable: particle data storage is unchanged from GADGET-2, tree storage is increased by $\sim 0.3(D-1)$, and Fourier storage requirements are unchanged. We subject the code to numerous tests to gauge performance both in runtime and in force accuracy. We verify that runtime is dominated by tree performance and scales as κD for $\kappa \in (1, 1.43)$ relative to that of GADGET-2. We find qualitatively identical, slightly improved, force accuracies compared to GADGET-2: behavior expected from our particular implementation. We also have introduced and verified a novel feature, which tracks the number of contributing particles of all species to any given monopole approximation, which can then be

Figure 6: Internal check of *ngravs* $N_\perp$ feature. Force accuracy comparison in pure tree mode between two distinct gravitationally interacting species: one Newtonian, the other as described with $\beta \equiv 1.31 \times 10^{-6}$. Note that force accuracy comparable to GADGET-2 is maintained when the number of particles contributing to monopole approximations, $N_\perp$, is tracked (yellow, solid) and used to adjust the force. Without such tracking, the force errors increase by an order of magnitude (orange, dashed).



used to correct exotic force laws with dynamic softening lengths. We believe that the *ngravs* extension will facilitate investigation and constraint of exotic gravitational scenarios and have released *ngravs* publicly[1] to the research community.

Acknowledgments

The author would like to thank Naoki Yoshida and Junichi Yokoyama for hospitality and encouragement, Volker Springel for warm and thorough feedback, and Larry Glasser for the elegant integration procedure leading to Eqn. (15). The author additionally thanks Tom Browder, Manuel Hohmann, and Brandon Wilson for useful discussions during code review. Significant portions of this work were performed at the Kavli Institute for Physics and Mathematics of the Universe (IPMU) and The University of Tokyo Research Center for the Early Universe (RESCEU) under joint support from National Science Foundation (NSF) Grant 1415111 and the Japan Society for the Promotion of Science (JSPS). Additional work was performed at the University of Tartu Institute of Physics, supported by the US Department of State under a Fulbright Student Award.

Appendix A. Initial conditions and simulation parameters

For completeness, we characterize the initial conditions and paired simulation parameters packaged with GADGET-2, which we have used to test and benchmark *ngravs*. These initial conditions were chosen for convenience and consistency, and they exercise the full range of modified functionality within *ngravs*. For simulations involving $D > 1$, collisionless particles were distributed evenly into the remaining types and assigned identical parameters.

[1]The website for downloading *ngravs* is https://github.com/kcroker/Gadget-2.0.7-ngravs

Table A.2: Initial conditions and parameters for the Pure Tree test case. ϵ is the softening length.

Collision of 2 spiral galaxies	
$\lvert x_i \rvert$	< 200 kpc
$\lvert v_i \rvert$	< 350 km/s
Type #1	Collisionless
	$N = 4 \times 10^4$
	$m = 1.05 \times 10^{-3}\ M_\odot$
	$\epsilon = 1$
Type #2	Collisionless
	$N = 2 \times 10^4$
	$m = 2.33 \times 10^{-4}\ M_\odot$
	$\epsilon = 0.4$

Table A.3: Initial conditions and parameters for the TreePM test case. Cosmological fractions and Hubble parameter are the standard values. ϵ is both the comoving and physical softening length, which was changed from an erroneous default value that caused the softening scale to overlap the PM transition region.

ΛCDM Universe from $z = 10$	
$\lvert x_i \rvert$	$< 5 \times 10^4$ kpc
$\lvert v_i \rvert$	$< 10^3$ km/s
Type #1	Collisional
	$N = 2^{15}$
	$m = 4.24\ M_\odot$
	$\epsilon = 50$
Type #2	Collisionless
	$N = 2^{15}$
	$m = 27.5\ M_\odot$
	$\epsilon = 50$

References

[1] Scott Dodelson. *Modern Cosmology*. Academic Press, 2003.
[2] D. Clowe, M. Bradač, A. H. Gonzalez, M. Markevitch, S. W. Randall, C. Jones, and D. Zaritsky. ApJ , 648:L109–L113, September 2006.
[3] Gianfranco Bertone, Dan Hooper, and Joseph Silk. *Phys.Rept.*, 405:279–390, 2005.
[4] LUX Collaboration. *ArXiv e-prints*, December 2015.
[5] C. P. Ahn, R. Alexandroff, C. Allende Prieto, S. F. Anderson, T. Anderton, B. H. Andrews, É. Aubourg, S. Bailey, E. Balbinot, R. Barnes, and et al. ApJS , 203:21, December 2012.
[6] G. Hinshaw, D. Larson, E. Komatsu, D. N. Spergel, C. L. Bennett, J. Dunkley, M. R. Nolta, M. Halpern, R. S. Hill, N. Odegard, et al. ApJS , 208:19, October 2013.

Table A.4: Initial conditions and parameters for the gas collapse profiling run. Note that masses are specified per particle in this initial condition.

Collapsing gas sphere	
$\lvert x_i \rvert$	0.1 cm
$\lvert v_i \rvert$	$= 0$
Type #1	Collisional
	$N = 1472$
	$m_i = 6.79 \times 10^{-4}$ g
	$\epsilon = 0.004$

[7] Planck Collaboration, P. A. R. Ade, N. Aghanim, C. Armitage-Caplan, M. Arnaud, M. Ashdown, F. Atrio-Barandela, J. Aumont, C. Baccigalupi, A. J. Banday, and et al. A&A , 571:A16, November 2014.

[8] R. W. Hockney and J. W. Eastwood. *Computer Simulation Using Particles*. IOP Publishing Ltd, 1988.

[9] J. S. Bagla and T. Padmanabhan. *Pramana*, 49:161, August 1997.

[10] V. Springel, S. D. M. White, A. Jenkins, C. S. Frenk, N. Yoshida, L. Gao, J. Navarro, R. Thacker, D. Croton, J. Helly, J. A. Peacock, S. Cole, P. Thomas, H. Couchman, A. Evrard, J. Colberg, and F. Pearce. *Nature*, 435:629–636, June 2005.

[11] Shy Genel, Mark Vogelsberger, Volker Springel, Debora Sijacki, Dylan Nelson, Greg Snyder, Vicente Rodriguez-Gomez, Paul Torrey, and Lars Hernquist. MNRAS , 445(1):175–200, 2014.

[12] M. Hohmann and M. N. R. Wohlfarth. Phys. Rev. D, 81(10):104006, May 2010.

[13] V. Springel. MNRAS , 364:1105–1134, December 2005.

[14] M. Baldi, V. Pettorino, G. Robbers, and V. Springel. MNRAS , 403:1684–1702, April 2010.

[15] E. G. Adelberger, B. R. Heckel, and A. E. Nelson. *Annual Review of Nuclear and Particle Science*, 53:77–121, December 2003.

[16] Kurt Hinterbichler. *Rev. Mod. Phys.*, 84:671–710, May 2012.

[17] A. Klypin, A. V. Kravtsov, O. Valenzuela, and F. Prada. ApJ , 522:82–92, September 1999.

[18] W. J. G. de Blok. *Advances in Astronomy*, 2010, 2010.

[19] Clifford M. Will. *Living Reviews in Relativity*, 9(3), 2006.

[20] V. Springel, N. Yoshida, and S. D. M. White. New A, 6:79–117, April 2001.

[21] Walter Dehnen and Justin I Read. *The European Physical Journal Plus*, 126(5):1–28, 2011.

[22] C. Power, J. F. Navarro, A. Jenkins, C. S. Frenk, S. D. M. White, V. Springel, J. Stadel, and T. Quinn. MNRAS , 338:14–34, January 2003.

[23] L. Hernquist, F. R. Bouchet, and Y. Suto. ApJS , 75:231–240, February 1991.

[24] M. L. Glasser and I.J. Zucker. *Theoretical Chemistry: Advances and Perspectives*, 5, 1980.

[25] R. E. Johnson and S. Ranganathan. Phys. Rev. E, 75(5):056706, May 2007.

[26] Matteo Frigo and Steven G. Johnson. *Proceedings of the IEEE*, 93(2):216–231, 2005. Special issue on "Program Generation, Optimization, and Platform Adaptation".

[27] S. Marri and S. D. M. White. *Monthly Notices of the Royal Astronomical Society*, 345(2):561–574, 2003.

[28] C. Scannapieco, P. B. Tissera, S. D. M. White, and V. Springel. *Monthly Notices of the Royal Astronomical Society*, 371(3):1125–1139, 2006.

[29] G. Salin and J.-M. Caillol. J. Chem. Phys., 113:10459–10463, December 2000.

[30] M. G. Walker, M. Mateo, E. W. Olszewski, J. Peñarrubia, N. Wyn Evans, and G. Gilmore. ApJ , 704:1274–1287, October 2009.